

Hotspot Analysis of Vegetation Fires and Intensity in the Indian Region

Krishna Prasad Vadrevu, Ivan Csiszar, Evan Ellicott, Louis Giglio, K. V. S. Badarinath, Eric Vermote, and Chris Justice

Abstract—In this study, we quantify vegetation fire activity in India using the MODerate resolution Imaging Spectroradiometer (MODIS) active fire datasets. We assessed different fire regime attributes, i.e., fire frequency, seasonality, intensity and the type of vegetation burnt in diverse geographical regions. MODIS data from 2002–2010 revealed an average of 63696 fire counts per year with the highest during 2009. Fire season in India extends from October to June with the peak during March. The K-means algorithm identified hotspot regions of fire clusters in diverse regions of India. We examined fire radiative power (FRP) data in the hotspot regions to address which fires burn intensively than others based on the vegetation type. We first assessed the best statistical fit distributions for the FRP data using the probability density functions (PDFs) and ranked them based on Kolmogorov-Smirnov statistic. We then described the fire intensities using empirical cumulative distribution functions (CDFs). Results suggest diverse pdfs for the FRP data that included Burr, Dagum, Johnson as well as Pearson distribution and they varied based on the vegetation type burnt. Analysis from empirical CDFs suggested relatively high fire intensity for closed broadleaved evergreen/ semi-deciduous forests than the other vegetation types. Although, annual sum of FRP for agricultural fires was less than the closed broadleaved evergreen forests, the values were higher than the mosaic vegetation category and broadleaved deciduous forests. These results on fire hotspots and FRP will be useful to address the impact of vegetation fires on air pollution and climate in India.

Index Terms— Fires, FRP, India, vegetation.

I. INTRODUCTION

VEGETATION fires are spread in the diverse biomes in both ‘natural’ and managed ecosystems [1]–[3]. Fire may profoundly alter the structure of the landscape [4], [5] and can affect ecological processes and function [6]–[8]. In addition, fires can cause complete destruction of vegetation cover and can impact plant composition, hydrological processes and rates

Manuscript received December 22, 2011; revised February 09, 2012 and April 19, 2012; accepted July 17, 2012. Date of publication September 14, 2012; date of current version March 11, 2013. This work was supported by NASA grant NNX10AU77G.

K. P. Vadrevu, E. Ellicott, E. Vermote, and C. Justice are with the Department of Geographical Sciences, University of Maryland, College Park, MD 20742 USA.

I. Csiszar is with the Satellite Meteorology and Climatology Division, NOAA/NESDIS Center for Satellite Applications and Research, Camp Springs, MD 20746 USA.

L. Giglio is with the Department of Geographical Sciences, University of Maryland, College Park, MD 20742 USA. He is also with the NASA Goddard Space Flight Center, Greenbelt, MD 20771 USA.

K. V. S. Badarinath was with the National Remote Sensing Center, Department of Space, Government of India, Hyderabad, India.

Color versions of one or more of the figures in this paper are available online at <http://ieeexplore.ieee.org>.

Digital Object Identifier 10.1109/JSTARS.2012.2210699

of soil erosion [9], [10]. Further, repeated burning can also modify the nutrient balance of soils, especially through the process of pyro-denitrification [11]. Outdoor fires, such as from wildfires and agricultural residue burning can emit particulate matter (PM) and other pollutants into the atmosphere impacting the air quality at both local and regional scales [11]–[14]. Quantifying the impact of fires on the environment requires information at multiple spatial scales.

One of the important concepts useful for addressing fire characteristics at a wide variety of scales is the fire regime. The fire regime of an area is defined by its fire type, fire intensity, severity, fire size, seasonality, spatial pattern, etc. [15], [16], [52], [53]. Use of vegetation fire statistics including records of ignition sources and the number of fire occurrences, is an effective method to quantify the temporal and spatial characteristics of fire regimes [17], [18]. A fire regime is the result of many interactions among physical and biophysical variables and can impact vegetation characteristics, species distribution, nutrient cycling, and ecosystem function [19], [20]. A fire regime is also dynamic due to the influences of climate conditions and human intervention [21]. Although purely natural fire regimes may not exist in the modern world, understanding of these fire regimes in time and space is still of great interest in both theory and practice [22].

Data on the fire regimes in the Indian region is scarce. It is estimated that nearly 3.73 Mha are burnt annually in India [23]. The fire season in India is severe during the dry season (March–May) and fire frequencies and intensities vary based on the vegetation type, climate conditions and socioeconomic factors. According to a State of the Forest Report [24], about 50% of the forested areas in India are fire prone. Apart from these general estimates, information on the number of fire occurrences, seasonality, hotspot regions of fire, type of vegetation burnt is not readily available. Understanding the impact of fires on vegetation and climate requires detailed knowledge about where fires occur, spatial and geographic gradients. For the same, satellite remote sensing technology with its synoptic coverage, multi-temporal, multi-spectral and repetitive capabilities provides robust information.

In this study, we used MODerate resolution Imaging Spectroradiometer (MODIS) active fire data to address the following questions pertinent to vegetation fires, in particular, their spatial distribution and fire intensity in India. How are the fire events distributed across different geographical regions? Are there any specific regions and ecosystems where fires cluster? Where are the hotspots? When is the peak fire season? What is the typical fire radiative power (FRP) of these fires? Are there any differences in FRP and annual sum of FRP released based on the vege-

tation type? Which statistical distribution most appropriately fit the FRP data, useful for modeling fire behavior?

In addition, we also tested two different hypotheses relating to annual sum of FRP (A-FRP). 1) Of the different forest types, A-FRP released from the closed broadleaved deciduous forests will be much higher compared to the closed to open broadleaved evergreen forests. The premise for this hypothesis is the broadleaved deciduous forests in India are characterized by warmer climates year-round and have long dry seasons which can last several months compared to evergreen forests. Thus, deciduous forests are highly fire prone and were hypothesized to have higher A-FRP values than the evergreen forests. The second hypothesis we tested pertains to agricultural residue burning. We hypothesized that 2) due to the lower fuel loads in agricultural systems compared to forests, the agricultural residue fires will have lower A-FRP values than the forest fires. From the questions and hypothesis addressed, the results from this study were expected to provide robust information on where fires occur, hotspot areas, fire-vegetation characteristics, fire intensity and the statistical nature of the fire intensity data useful for addressing fire management and mitigation options.

II. DATASETS AND METHODOLOGY

A. Active Fires, Fire Radiative Power (FRP), Annual Sum of FRP

We used the MODIS daily active fire product (MCD14ML) for spatial depiction, monthly FRP (MOD14CMH/MYD14CMH) product for characterizing the fire intensities in India. The FRP data are an aggregated daily datasets for individual months. The real-time active fire data are processed through MODAPS (MODIS Adaptive Processing System) and also available through FIRMS (Fire Information for Resource Management System) [25]. The MODIS two sun synchronous, polar orbiting satellites pass over the equator at approximately 10:30 am/pm (Terra) and 1:30 pm/am (Aqua) with a revisit time of 1 to 2 days. The data collected by the sensor is processed by MODAPS using the enhanced contextual fire detection algorithm [26] into the Collection 5 Active fire product. For this study, we analyzed the annual fires from 2002–2010 and specifically focused on 2010 fires for answering specific questions, when both the Terra and Aqua satellites were simultaneously collecting data. The fire data are at 1 km nominal spatial resolution at nadir, however, under ideal conditions flaming fires as small as 50 m² can be detected (<http://maps.geog.umd.edu/firms/faq.htm#size>).

FRP is the rate of fire energy released per unit time, measured in megawatts [27], [28]. FRE is FRP integrated over time and space and described in units of mega joules (MJ). The MODIS algorithm for FRP is calculated as the relationship between the brightness temperature of fire and background pixels in the middle infrared (band center near 4 μm). It is given as [27], [28]

$$FRP = 4.34 \times 10^{-19} (T_{MIR}^8 - T_{bg,MIR}^8) \quad (1)$$

where FRP is the rate of radiative energy emitted per pixel, 4.34×10^{-19} (MW km⁻² Kelvin⁻⁸) is the constant derived from the simulations, T_{MIR} (Kelvin) is the radiative brightness temperature of the fire component, $T_{bg,MIR}$ (Kelvin) is the

neighboring non-fire background component, and MIR refers to the middle infrared wavelength, typically 4 μm . In this study, we utilized the collection 5 Terra and Aqua monthly climate modeling grid datasets (MOD14CMH/MYD14CMH) [30] that represent cloud and over pass corrected fire pixels data along with the mean FRP data.

B. Vegetation Type

We used the land use/cover product from MERIS data at a 300 m resolution for characterizing the vegetation types [31] (Fig. 1). The land cover product is derived by classification of a time series of MERIS full resolution mosaics from December 2004–June 2006. Its 22 land cover global classes are defined with the United Nations Land Cover Classification System (LCCS). We used this product due to its high spatial resolution (300 m) compared to the other global land cover products. Specifically, the active fires from MODIS were overlaid on the MERIS vegetation map to analyze the fire regimes (frequency, extent, seasonality, type of vegetation burnt).

C. Cluster Analysis

For the MODIS fire data corresponding to the latest years (2010, 2011), we performed a cluster analysis to identify hotspots of fires in different geographical locations and vegetation types. Clustering is loosely defined as “the process of collecting objects into groups whose members are similar in some way” [32]. The goal of clustering is thus to determine the intrinsic grouping in a set of unlabelled data [33]. K-means clustering is one of the popular unsupervised learning algorithms [33]–[35]. An important characteristic of K-means approach is the use of centroids for grouping observations. The technique is based upon the multivariate analysis of variance in the evaluation of homogeneity among entities [36]. The k-means approach is represented as

$$\text{Minimize } Z = \sum_i \sum_k a_i d_{ik}^2 y_{ik} \quad (2)$$

Subject to

$$\sum_k y_{ik} = 1 \quad (3)$$

$$y_{ik} = 0, 1 \quad (4)$$

where ‘i’ is the index of observations; a_i is the attribute weight of observation (number of fires at a given location on our case); k = index of clusters; d_{ik} = distance between observation ‘i’ and cluster ‘k’; d_{ik} = distance between observation ‘i’ and cluster ‘k’; and

$$y_{ik} = \begin{cases} 1 & \text{if observation } i \text{ is assigned in cluster } k \\ 0 & \text{otherwise} \end{cases} \quad (5)$$

The K-means clustering algorithm partitions a given data set through a certain number of k clusters fixed *a priori*. Starting from a random initialization, the algorithm iterates two simple phases: takes each point belonging to a given data set and associates it with the nearest centroid and then, when no point is pending, re-computes the k new centroids as the barycenters of groups resulting from the previous step [34], [37]. After these k new centroids, new association phases are performed iteratively between the same data set points and the nearest new centroid.

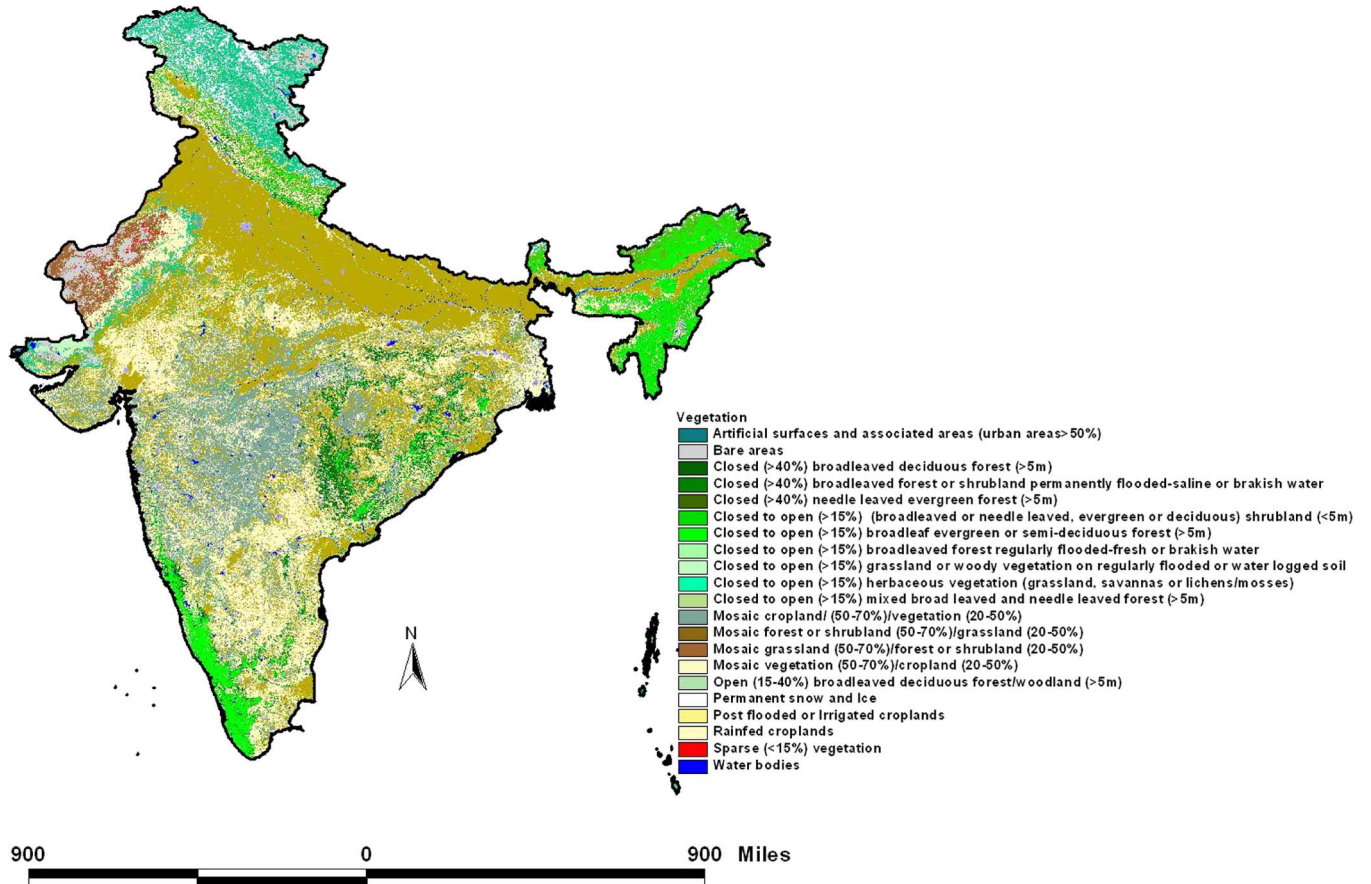


Fig. 1. MERIS derived vegetation map of India.

As a result of this loop, the k centroids change their location step by step until no more changes occur, i.e., the centroids do not move anymore [38], [39]. We restricted our clusters to eight to depict major biomass burning regions. Further, to identify the cluster locations, we used the standard deviation ellipses [39]. We typically used one standard deviation, i.e., each ellipse covering more than 50% of the clustered fire events. Previously, the K-means clustering algorithm is used in a wide variety of applications including data mining and data discovery [54], data compression and vector quantization [55] and pattern recognition and pattern classification [56]. More specifically, the algorithm has been used in marketing research [57], clustering urban crime patterns [58], disease transmission patterns [59], clustering gene expression [60], profiling road accident hotspots [61], etc. In this study we used it for identifying fire clusters during 2010 and 2011 over India using the MODIS dataset.

D. Descriptive Statistics

A 4×4 grid with a cell size of 0.5×0.5 degrees (total of $\sim 220 \times 220 \text{ km}^2$) is overlaid on each of the K-mean fire cluster ellipses (Fig. 3) and the underlying FRP values have been extracted (2010, 2011). We used a variety of descriptive statistics to assess the FRP values in the clusters which included number of fire counts, FRP minimum, maximum, range, 1st quartile, median, 3rd quartile, sum, mean, variance, standard deviation, coefficient of variation, skewness, mean absolute deviation and

median absolute deviation. In addition, we also evaluated the monthly FRP for the fire clusters for relative comparison.

E. FRP Distribution Fitting and Comparison

Distribution fitting is useful when the statistical origin and properties of a given data are unknown. Several distribution types are available to identify the correct origin of distribution. Fire clusters in our case were identified in a wide variety of geographical regions and ecosystem types. The underlying causative factors of fires in these clusters may be different, thus the associated FRP values. Quantifying the underlying statistical distributions of the FRP data may provide useful information on fire behavior and modeling. For a constant grid size and fire cluster data described earlier, using the 2010 sampled data, we assessed for the best statistical fit distributional forms using the probability density functions, cumulative distribution functions (CDFs) and the Quantile plots. We used Kolmogorov Smirnov (K-S) goodness of fit statistic to assess the relative effectiveness of the individual distributions and identifying the best-fit for the fire-cluster FRP data [40]. The K-S test is based on the largest vertical difference between $F(x)$, the theoretical distribution function, and $F_n(x) = (\text{number of observations} \leq x)/n$. The KS statistic for a given cumulative distribution function ($F(x)$) is given as

$$D_n = \sup_x |F_n(x) - F(x)| \quad (6)$$

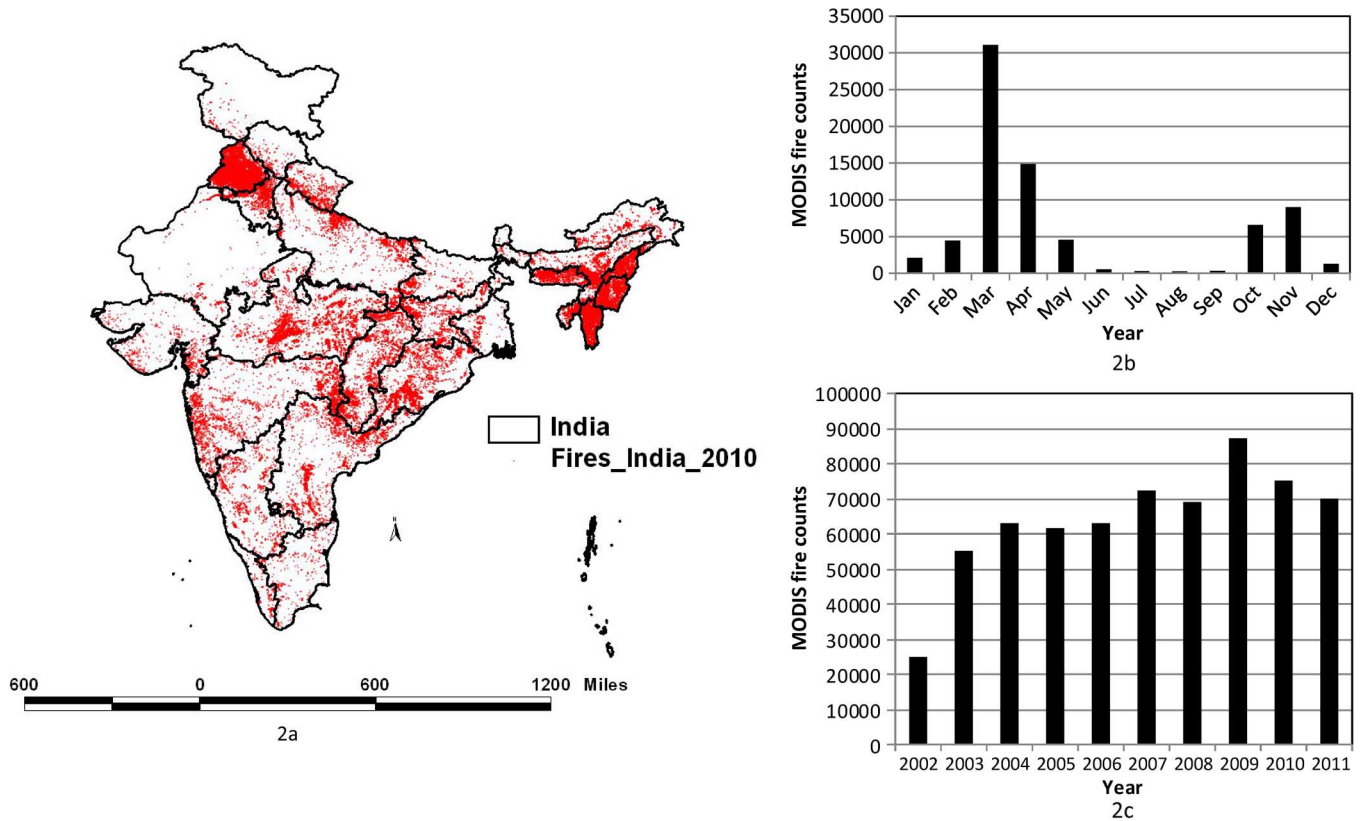


Fig. 2. (a) Spatial pattern in MODIS derived active fires for March 2010. (b) Fire seasonality (2010) with the peak fire activity during March; (c) Trends in fire activity for different years with the highest fire counts in 2009.

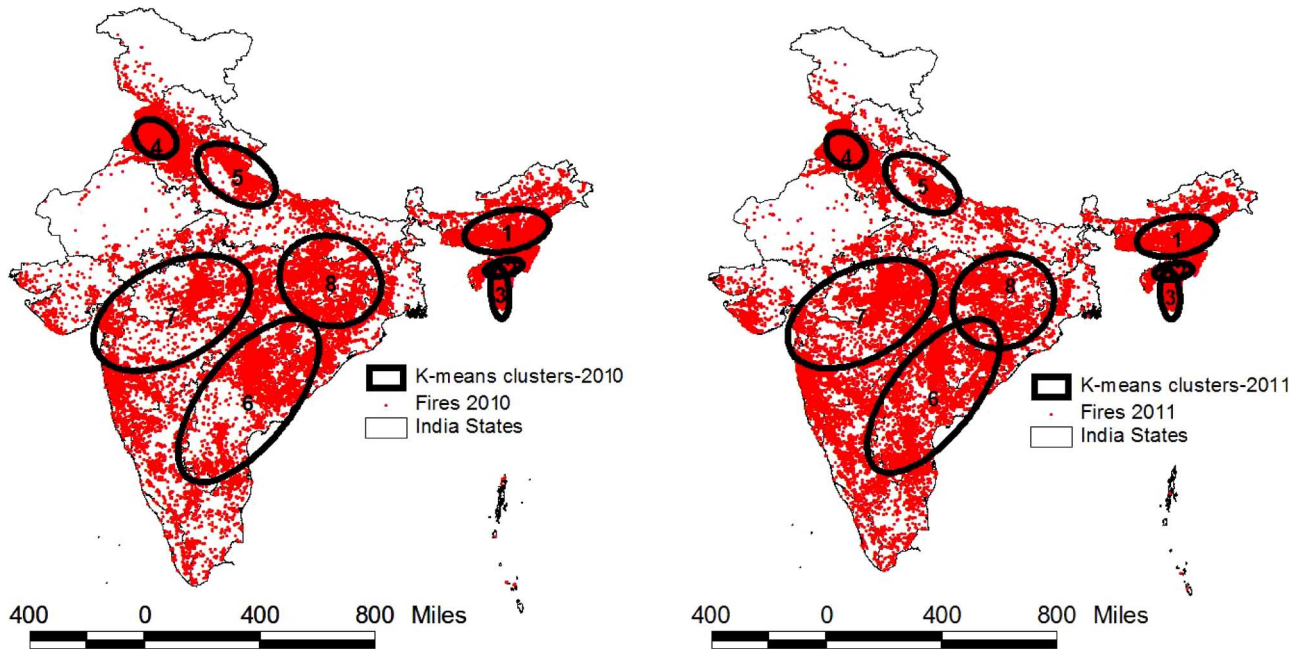


Fig. 3. Fire hotspots as identified by K-means clustering algorithm (2010, 2011).

where sup_x is the set of distances. K-S compares the empirical cumulative distribution function of the sample data with the distribution expected if the data were normal. If the observed difference is sufficiently large, the test will reject the null hypothesis of population normality. If the p-value of these test is less than the chosen alpha level (0.01 level in this study),

null hypothesis is rejected and concluded that the population is non-normal. After fitting the best probability distribution function, a Quantile-Quantile (Q-Q) plot was used to detect shifts in the location of FRP values, scale, symmetry and the presence of outliers. The Q-Q plot will be approximately linear if the specified theoretical distribution is the correct model. Further, em-

TABLE I
MODIS FIRE COUNTS (2010) AGGREGATED BASED ON MERIS (300 m) VEGETATION MAP

Vegetation type	% Fire counts
Post flooded or irrigated croplands (or aquatic)	35.375
Rainfed croplands	9.436
Mosaic cropland (50-70%)/vegetation (20-50%)	8.867
Mosaic vegetation (50-70%)/cropland (20-50%)	7.634
Closed to open (>15%) broadleaf evergreen or semi-deciduous forest (>5m)	13.663
Closed (>40%) broadleaved deciduous forest (>5m)	8.559
Open (15-40%) broadleaved deciduous forest/woodland (>5m)	0.188
Closed (>40%) needleleaved evergreen forest (>5m)	1.264
Open (15-40%) needleleaved deciduous or evergreen forest (.5m)	0.000
Closed to open (>15%) mixed broadleaved and needleleaved forest (>5m)	0.003
Mosaic forest or shrubland (50-70%)/grassland (20-50%)	0.016
Mosaic grassland (50-70%)/forest or shrubland (20-50%)	0.018
Closed to open (>15%) (broadleaved or needleleaved, evergreen or deciduous) shrubland (<5m)	13.886
Closed to open (>15%) herbaceous vegetation (grassland, savannas or lichens/mosses)	1.038
Sparse (<15%) vegetation	0.053
Total	100.0

TABLE II
HOTSPOT REGIONS OF FIRE CLUSTERS AS IDENTIFIED BY K-MEANS ALGORITHM

Cluster	Districts
Cluster-1	Hotspot districts in northeast India i.e., Nalbari, Nagaon, North Cacha hills in Assam, Tamenglong, Senapati, Ukhrul in Manipur, Ri Bhoi, West and East Khasi hills, Jaintia hills in Meghalaya, Dimapur, Phek, Wokha, Kohima in Nagaland, etc.
Cluster-2-3	Relatively smaller fire clusters in the districts of Aizal, Champhai, Kolasib, Mamit, etc in Mizoram, parts of Churachandpur in Manipur and North Tripura district in Tripura, etc.
Cluster-4	Fires in Punjab state covering most of the districts and Sirsa and Fatehbad in Harayana state, etc.
Cluster-5	Fire clusters in the Uttar Pradesh covering districts of Almora, Babeshwar, Barielly, Bijnor, Budaun, Bulandshahr, Etah, Farukhabad, Garhwal, Ghaziabad, etc .
Cluster-6	East Godavari, Warangal, Karimnagar, Mahbubnagar, Nalgonda and several other districts in Andhra pradesh state; Kanker, Raj Nandgaon, Durg, Rajpur, etc., districts in Chattisgarh, Tumkur and Kolar districts in Karnataka; Nabrangapur, Kalahandi, Balangir, Koraput and other districts in Orissa state, etc.
Cluster-7	Cluster 7 covered several districts including Indore, Sagar, Dewas, Jhabua, West Nimar, East Nimar, Ujjain, Ratlam, etc., in Madhya Pradesh state and Nandurbar, Nashik, Dhule, Buldana, Jalgoan, Akola, and other districts in Maharastra, etc.
Cluster-8	Highly diverse cluster eight and mostly focused over the eastern and central India covering districts of Bhabhua, Nalanda, Nawada, Gaya districts in Bihar state; Jashpur, Bilaspur, Korba, Koriya, etc in Chattisgarh state; Kodema, Garwa, Bokaro, Gumla etc in Jharkhand state; Sidhi in Madhya Pradesh; Sambalpur, Kendujhar in Orissa; Sonbhadra, Mirzapur, Chandauli in Uttar Pradesh, etc.

pirical distribution plots for each of the cluster data were used to assess the FRP differences.

III. RESULTS AND DISCUSSION

Spatial variation in fire counts based on MODIS active fire data for the year 2010 for India is shown in Fig. 2(a), monthly variations in Fig. 2(b) and yearly variations in Fig. 2(c). Of the different years, 2009 recorded the highest number of fires followed by 2007, 2010 and others. An average of 63696 fire counts per year is recorded in India. Fire season in India extends from October to June during which more than 70% of total fires are recorded with the peak during March with 41.2% of fires, April (19.7%), May (6.03%), etc. (Fig. 2(b)). Further, MODIS Aqua captured 73.3% of the fires relative to MODIS Terra with 26.6%, suggesting that most of the fires occur during the afternoon. Fire counts aggregated based on the MERIS (300 m)

derived vegetation map (Fig. 1) for the year 2010 for the entire India is given in Table I. While aggregating the fire counts, non-vegetation classes such as regularly flooded areas, urban areas, bare areas, water bodies and permanent snow and ice categories were removed. Results suggested that of all the categories, irrigated croplands has the most fire counts (35%) followed by closed to open shrubland category (13.88%), closed to open broadleaf evergreen or semi-deciduous forest (13.63%), etc.

Results on the fire-vegetation analysis (Tables I, II) suggests that a variety of vegetation types are burnt in diverse geographical regions. K-means clustering algorithm was useful in identifying fire hotspots in diverse geographical regions (Fig. 3, Table II). The hotspot map generated through K-means clustering allowed easier interpretation of fire clusters and their geographical location. There was not much difference in the

TABLE III
FIRE COUNTS (IN PERCENT) WITHIN A 220 × 220 sq.km MESH AGGREGATED BASED ON THE MERIS VEGETATION TYPES. THE DOMINANT VEGETATION TYPES ARE HIGHLIGHTED IN BOLD

Vegetation type	Cluster_1	Cluster_2_3	Cluster_4	Cluster_5	Cluster_6	Cluster_7	Cluster_8
Post-flooding or irrigated croplands (or aquatic)	3.0	0.1	99.3	41.7	2.0	66.2	13.8
Rainfed croplands	2.4	1.6	0.1	9.4	9.4	13.2	19.1
Mosaic cropland (50-70%) / vegetation (grassland/shrubland/forest) (20-50%)	0.5	0.6	0.4	1.2	9.7	17.6	30.5
Mosaic vegetation (grassland/shrubland/forest) (50-70%) / cropland (20-50%)	15.0	6.2	0.2	12.6	6.4	1.8	9.0
Closed to open (>15%) broadleaved evergreen or semi-deciduous forest (>5m)	70.5	41.3	0.0	7.5	8.4	0.0	9.0
Closed (>40%) broadleaved deciduous forest (>5m)	0.2	1.4	0.1	14.5	58.8	0.3	18.1
Open (15-40%) broadleaved deciduous forest/woodland (>5m)	0.1	1.2	0.0	0.0	0.0	0.0	0.0
Closed (>40%) needleleaved evergreen forest (>5m)	2.8	1.5	0.0	3.1	0.0	0.0	0.0
Closed to open (>15%) mixed broadleaved and needleleaved forest (>5m)	0.0	0.0	0.0	0.1	0.0	0.0	0.0
Mosaic forest or shrubland (50-70%) / grassland (20-50%)	0.0	0.0	0.0	0.0	0.0	0.0	0.0
Mosaic grassland (50-70%) / forest or shrubland (20-50%)	0.0	0.0	0.0	0.0	0.0	0.0	0.0
Closed to open (>15%) (broadleaved or needleleaved, evergreen or deciduous) shrubland (<5m)	5.4	46.1	0.0	9.8	3.7	0.0	0.5
Closed to open (>15%) herbaceous vegetation (grassland, savannas or lichens/mosses)	0.0	0.0	0.0	0.3	1.6	0.9	0.0
Sparse (<15%) vegetation	0.0	0.0	0.0	0.0	0.0	0.0	0.0
Closed to open (>15%) broadleaved forest regularly flooded (semi-permanently or temporarily) - Fresh or brackish water	0.0	0.0	0.0	0.0	0.0	0.0	0.0
Closed (>40%) broadleaved forest or shrubland permanently flooded - Saline or brackish water	0.0	0.0	0.0	0.0	0.0	0.0	0.0
Closed to open (>15%) grassland or woody vegetation on regularly flooded or waterlogged soil - Fresh, brackish or saline water	0.0	0.0	0.0	0.0	0.0	0.0	0.0
Sum	100	100	100	100	100	100	100

2010 versus 2011 fire clusters except that the standard deviation ellipse of cluster 8 during 2011 slightly overlapped with cluster 6. To capture the fire events and associated FRP values within a specific vegetation category, we used the MERIS derived vegetation map. Further, as the clusters identified by the K-means algorithm were quite different from each other, to get an unbiased estimate pertaining to the area covered, we used the same 4 × 4 grid with a cell size of 0.5 × 0.5 degrees as above. Fire counts aggregated based on the vegetation type information for the individual clusters in percentage is shown in Table III. We aggregated clusters two and three (Fig. 3) as the combined area covered by these clusters is less than the selected grid size for analysis. FRP values associated with the fire incidences strongly depend on the type of fuel material burnt. The vegetation types identified using the MERIS data suggested that closed to open broadleaved evergreen or semi-deciduous forest category and closed to open shrubland category in the north-east India (cluster-1 and 2–3) had the second highest fire counts. In these clusters, the vegetation is dominated by mostly evergreens or semi-deciduous species such as *Chukrasia tabularis*, *Calophyllum polyanthum*, *Elaeocarpus tectorius*, *Litsea lancifolia*, *Syzygium cuminii*, *Terminalia myriocarpa*, etc. [62]. The vegetation is also dominated by Bamboo. In general, these species are not conducive for quick ignition due to high moisture content. Large amount of fires in the region are attributed to slash and burn agriculture also known as Jhum, practiced by the local indigenous people [43], [44]. Jhum is practiced by the farmers of upland communities of northeast India and over 400,000 families. The average land holding under jhum cultivation varies from 0.16–1.3 ha per family. Mixed cropping with a fallow period of 3–10 years is the main characteristic of the system. The forests are cleared during late December/January and the slash is burnt starting February till May. The peak burning occurs during March (Fig. 4(d), (f)). The sowing operations are then carried out prior to the onset of pre-monsoon and monsoon rains.

In contrast to cluster 1, 2–3, fires in cluster 4 (Fig. 4(b)) of Punjab region are attributed to agricultural residue burning [42]. Of the total cropped areas, rice occupies 37.15% and wheat occupies 48.76%, and these crops together constitute 85.91% of grown crops. The other crops such as maize, jowar, cotton,

pulses, vegetables, etc., constitute only 14% of the total cropped area. In this region, rice is usually grown in the wet summer season (sowing-May–June and harvesting-October–November) and wheat in the dry winter season (sowing-November–December and harvesting-March till May). Farmers mostly use combines for harvesting the rice and wheat. Although effective, for most part, combines leave large amount of residues after harvest. To clear the land for next crop farmers burn the leftover residues on field (open burning) [41]. The reasons for burning of agricultural residues in the study area can be summarized as follows: a) Manual harvesting and threshing of rice/wheat involve high labor costs; b) Use of Combines allows rapid field preparation for the next crop, however, it leaves large amount of residues on field; c) Use of rice residues as cattle feed is not so common although wheat residues were fed, before combine harvesters came to practice; d) There is no significant income generating alternate use of rice residues; e) Burning residues is a quicker way to clear the fields for the next crop. Thus, in this region, fires follow a bimodal pattern in a single year (Fig. 4(b)). Similar trend is shown by fires in the Cluster-5 region (Fig. 4(c)), although with a relatively lower number of fires, as this region is also a part of Indo-Ganges region dominated by the agriculture (Table II), mainly Rice-Wheat cropping system and the crop residue burning [42]. Further, in this region, the peak burning that occurs during April is attributed to burning of closed broad leaf deciduous forests (Table III) [63].

Fires in cluster 6 (Fig. 4(g)) dominated in the Andhra Pradesh and Orissa border states are mainly attributed to slash and burn agriculture, locally known as “Podu” [64]. The vegetation is dominated by closed broad leaved deciduous forest with the species of *Xylia xylocarpa*, *Terminalia alata*, *Anogeissus latifolia*, etc. Similar to forested regions of north India, the region is inhabited by indigenous people who practice “Podu” cultivation. In this region, peak fires occur during the March, summer season. Biomass that is clear felled during the late winter (December) is burnt from January–June. The burning starts early (January–February) in the lower elevation regions while late burning (March–June) occurs in the high elevated regions. Fires in the cluster-7 (Fig. 4(e)) in the Madhya Pradesh and Maharashtra state are attributed to biomass burning of

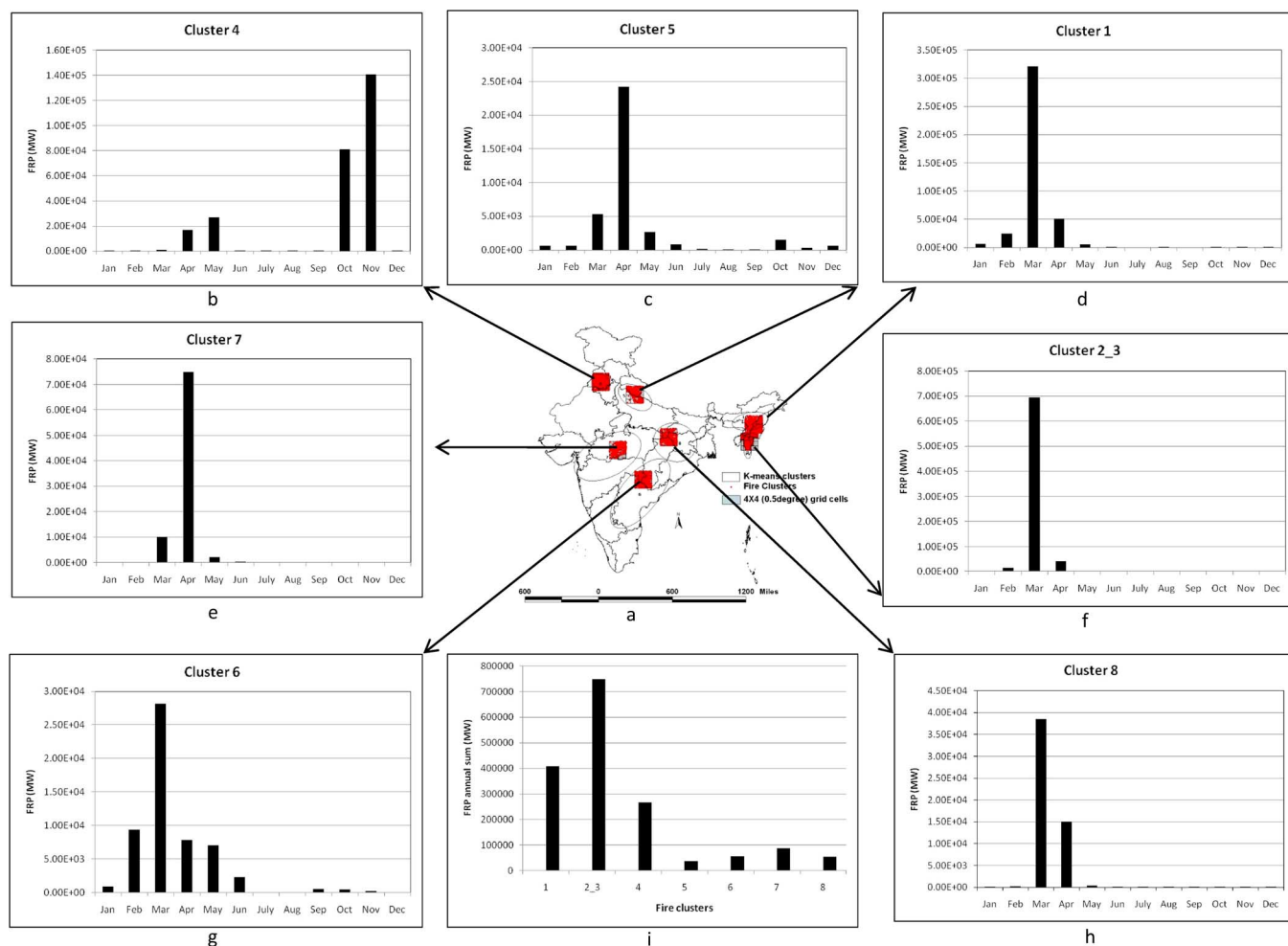


Fig. 4. (a) India map with fire clusters in a 220×220 sq.km mesh; (b)–(h) Monthly FRP in different fire clusters; (i) Annual sum of FRP in different fire clusters. See Table I for vegetation characteristics underlying these fire clusters.

crop residues, mostly Soybean and Wheat. In addition to crop burning, forest burning is also common due to intentional fires of tropical deciduous forests. The forests are burnt for clearing of land for agriculture, facilitating growth of grass for cattle grazing, in addition to management fires by the local forest department. Cluster-8 with fires occurring in the different states of Jharkand, Madhya Pradesh and Uttar Pradesh state (Fig. 4(h)) are attributed to forest as well as agricultural residue burning. Vegetation analysis (Table II) suggested that in this region, fires occurred mostly in the mosaic vegetation and mosaic cropland category.

Our analysis suggests K-means clustering as an effective technique for identifying fire hotspots from satellite inputs. The results can be useful for fire management purposes both in terms of risk evaluation and post-fire impacts on ecosystem services. Most importantly, the decisions that fire managers and planners make depend on the spatial characteristics of fires. For example, pre-suppression decisions are often aimed at allocation of firefighting funds, personnel and equipment [49]. The results obtained on fire characteristics, their geographical locations and vegetation types should help resource managers and environmental scientists to identify potential hotspot areas where fire management efforts can be focused.

Further, the spatial patterns of fire clusters can be useful to address questions relating to causative factors (vegetation type, meteorology, human impacts) and impacts (air pollution, vegetation disturbance, etc).

Descriptive statistics for the individual fire clusters for 2010 and 2011 are listed in Table IV. Of the different clusters, cluster 4 that is located in Punjab had the highest number of fire counts followed by clusters 2–3 and cluster 1 corresponding to north-east India, followed by cluster 7 (mean for two years) in south India and others. Large numbers of fire counts in Punjab are due to agricultural residue burning that occurs in very small fields. Although the fire counts were highest in cluster 4, several other attributes for the FRP such as the maximum, mean, sum, variance, standard deviation, coefficient of variation, skewness, mean absolute deviation as well as median absolute deviation of FRP were considerably higher for cluster 2–3 and 1 in north-east India than cluster 4 and others (Table IV). These differences suggest variations in the type of evergreen forest biomass burnt in cluster 2–3 compared to homogenous agricultural biomass residues burnt from either rice or wheat in cluster 4. Interestingly, the FRP values in cluster 4 corresponding to agricultural fires had a relatively higher sum of FRP than fire cluster 6 dominated by closed broadleaf deciduous forests. Cluster 7 domi-

TABLE IV
SUMMARY STATISTICS FOR THE FRP VALUES IN A 220 × 220 sq.km MESH WITHIN THE FIRE CLUSTERS (2010, 2011)

FRP Statistics (2010)	Cluster 1	Cluster 2_3	Cluster 4	Cluster 5	Cluster 6	Cluster 7	Cluster 8
Mean	70.11	103.68	19.59	25.04	24.29	45.30	30.25
No. of fire counts	4997.00	6471.00	11540.00	935.00	1976.00	1158.00	1464.00
Minimum	4.70	3.20	4.20	5.10	5.20	6.40	5.40
Maximum	2202.30	4643.30	192.80	189.60	464.60	583.30	477.60
Range	2197.60	4640.10	188.60	184.50	459.40	576.90	472.20
1st Quartile	16.10	19.20	10.60	12.10	12.28	16.80	13.90
Median	30.90	40.50	15.30	17.20	17.60	27.40	21.20
3rd Quartile	67.60	94.70	23.80	28.75	27.23	52.28	35.00
Sum	350340.50	670916.00	226018.30	23413.30	47993.60	52458.70	44281.00
Variance (n)	18390.66	54761.81	198.59	540.31	683.82	2578.32	978.69
Standard deviation (n)	135.61	234.01	14.09	23.24	26.15	50.78	31.28
Variation coefficient	1.93	2.26	0.72	0.93	1.08	1.12	1.03
Mean absolute deviation	65.19	103.68	9.68	14.67	13.42	32.17	17.90
Median absolute deviation	18.30	26.10	5.70	6.60	6.50	13.20	8.60

FRP Statistics (2011)	Cluster 1	Cluster 2_3	Cluster 4	Cluster 5	Cluster 6	Cluster 7	Cluster 8
Mean	82.42	106.98	20.67	22.60	35.45	36.97	19.14
No. of fire counts	3395	4024.00	14009.00	940.00	1676.00	3091.00	984.00
Minimum	5.30	4.20	4.10	0.82	5.20	4.20	5.20
Maximum	2985.10	2038.90	226.30	239.70	1777.80	670.70	159.70
Range	2979.80	2034.70	222.20	239.70	1772.60	666.50	154.50
1st Quartile	18.10	22.80	11.00	10.90	12.50	13.90	10.60
Median	35.45	50.20	16.00	15.80	18.70	21.70	19.50
3rd Quartile	82.53	118.05	25.00	25.80	33.13	39.80	22.50
Sum	331691.90	363225.70	289531.30	21252.60	59406.90	114283.90	18831.70
Variance (n)	23681.67	28087.53	234.61	417.84	5356.66	2177.71	209.13
Standard deviation (n)	153.89	167.59	15.32	20.44	73.19	46.67	14.46
Variation coefficient	1.87	1.57	0.74	0.90	2.06	1.26	0.76
Mean absolute deviation	76.81	96.29	10.42	13.26	28.40	26.87	9.28
Median absolute deviation	21.65	34.40	6.20	6.30	7.70	9.60	4.90

nated by irrigated croplands and mosaic cropland category in Central India had higher sum of FRP values than the cluster 6 dominated by the closed broadleaf deciduous forests. FRP density (per square mile) based on the standard deviation classification stretch is shown with a multicolor color ramp (Fig. 5). Standard deviations are useful in defining where in a distribution the cut off is between values of different statistical significance. In Fig. 5, blue indicates standard deviation above the mean and the more intense colors from green to orange shows increasing deviation. White shows standard deviation below the mean. Thus, the FRP density in the northeast India as well as Punjab had the highest standard deviation suggesting the relative spread of data compared to the other regions. The standard deviation stretch

of the FRP values matched the spatial patterns of fire hotspots identified by the K-means clustering algorithm. However, as the FRP data was hypothesized to be non-normally distributed, in addition to standard deviation stretch, we evaluated the other robust statistical measures to address fire-related questions.

The PDFs fitted for the FRP clusters (2010) along with the best fit distributions ranked based on the K-S statistic, parameter and p-values is given in Table V. Probability density function plots as well as quantile-quantile (Q-Q) plots were shown for the top-ranked best-fit distributions for the individual FRP fire clusters in Fig. 6. A distribution that is confined to lie between two determined values is said to be bounded. A general observation of the limits of the FRP top-ranked best-fit distributions

TABLE V
BEST STATISTICAL DISTRIBUTION FITS AND PARAMETERS FOR THE FRP DATA IN DIFFERENT CLUSTERS RANKED AS PER THE KOLMOGOROV-SMIRNOV STATISTIC

Fire cluster	Distribution and Parameters	Rank	K-S statistic	
			Statistic	P-value
1	Burr (4P) ($k=0.25793$ $\alpha=3.612$ $\beta=13.486$) Inverse Gaussian (3P) ($\lambda=18.735$ $\mu=70.11$) Pearson 6 (4P) ($\alpha_1=2.8297$; $\alpha_2=1.2814$; $\beta=9.9456$; $\gamma=4.5577$)	1	0.70423	0.37949
		2	2.688	0.03269
		3	4.745	0.01334
2_3	Burr-4P ($k=0.33244$; ($\alpha=4.8272$; $\beta=11.4$) Inverse Gaussian (3P) ($\lambda=29.312$ $\mu=110.84$ $\gamma=3.3577$) Log-normal (3P) ($\sigma=1.153$; $\mu=3.9303$)	1	0.0110	0.5663
		2	0.0158	0.16282
		3	0.01643	0.1331
4	Johnson SB ($\gamma=4.5962$; $\delta=1.1049$; $\lambda=594.35$; $\xi=5.4487$) Pearson 6 (4P) ($\alpha_1=5.4181$; $\alpha_2=3.1784$; $\beta=6.0521$; $\gamma=3.898$) Pearson 5 (3P) ($\alpha=2.8993$; $\beta=32.403$; $\gamma=2.0204$)	1	0.0168	0.144
		2	0.0177	0.086
		3	0.01836	0.06804
5	Dagum ($k=56.709$; $\alpha=1.8869$; $\beta=1.6964$) Pearson 5 (3P) ($\alpha=2.2597$ $\beta=30.094$ $\gamma=2.0699$) Frechet (3P) ($\alpha=1.9296$ $\beta=14.397$)	1	0.01892	0.885
		2	0.01952	0.861
		3	0.0196	0.85806
6	Log-Pearson 3 ($\alpha=4.2144$; $\beta=0.29725$; $\gamma=1.7026$) Pearson 6 (4P) ($\alpha_1=8.3275$; $\alpha_2=2.4098$; $\beta=3.3931$; $\gamma=4.4191$) Pearson 5 (3P) ($\alpha=2.3407$; $\beta=28.765$; $\gamma=3.1183$)	1	0.0115	0.952
		2	0.0148	0.771
		3	0.0153	0.733
7	Burr (4P) - ($k=0.23655$; $\alpha=4.9468$; $\beta=14.2$) Inverse Gaussian - (3P) ($\lambda=36.026$; $\mu=45.301$) Gen. Pareto - ($k=0.30578$; $\sigma=25.251$; $\mu=8.928$)	1	0.0203	0.715
		2	0.0209	0.681
		3	0.0264	0.39586
8	Burr (4P) - ($k=0.28765$; $\alpha=5.2337$; $\beta=12.867$) Pearson 6 (4P) - ($\alpha_1=6.8627$; $\alpha_2=2.2691$; $\beta=4.9327$; $\gamma=4.4946$) Pearson 5 (3P) - ($\alpha=2.1785$; $\beta=33.846$; $\gamma=2.7176$)	1	0.01231	0.977
		2	0.02629	0.246
		3	0.02641	0

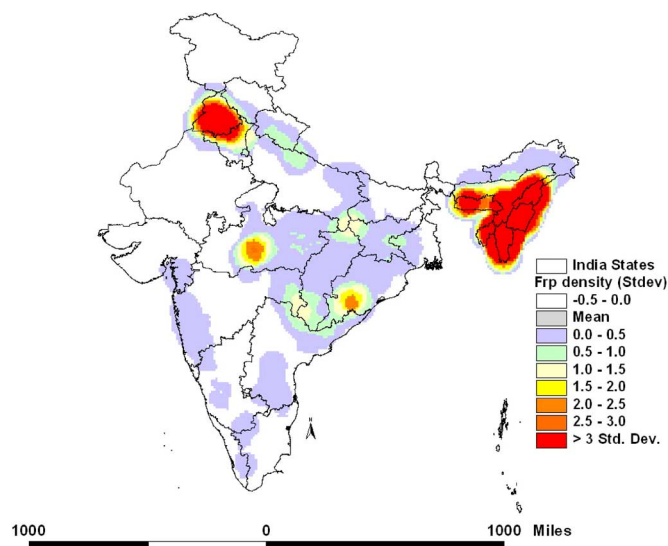


Fig. 5. FRP density (per sq.mile) classified using standard deviation stretch.

suggests that all of them pertained to the bounded type. The best fit FRP distribution for clusters 1, 2–3, 7 and 8 was found to be a Burr distribution (Fig. 6). The best fit for the FRP data dominated by agricultural fires (cluster 4) was found to be Johnson SB which is both a left-and right bounded distribution. This is justified, as agricultural fires showed a clear bi-modal distribu-

tion during summer and winter (Fig. 4(b)) [42]. For cluster 5 dominated by the irrigated croplands and closed broadleaf deciduous forests, Dagum distribution is found to be the best fit for the FRP data whereas for the FRP data in cluster six dominated by the broadleaf deciduous forests, Log Pearson-3 distribution was found to be the best fit (Fig. 6). Log Pearson-3 is similar to normal distribution, except instead of two parameters, standard deviation and mean, it also has a skew. When the skew is small, Log Pearson Type III distribution approximates normal. The Q-Q plots for the FRP data values plotted against the theoretical (fitted) distribution FRP (in MW) quantiles is shown beside the pdf plots. The Q-Q plots were linear for more than ninety percent of the data points suggesting that the theoretical distribution fitted well. These results on the best-fit statistical distributions of FRP data can be incorporated into simulation models for quantifying fire behavior, spread and risk. The results can also be integrated with atmospheric transport models to assess pollutant behavior and climate impacts in diverse landscapes. Statistical distributions are the key for understanding the behavior of data and FRP showed wide variability based on the type of fires (eg: agricultural fires versus forest) and geographical regions. Since research relating to FRP is leading to emissions estimation, our results from statistical distributions of FRP suggests that regionally fine-tuned models based on FRP statistical distributions and emissions might yield better estimates.

The empirical cumulative distribution function (cdf) plots for the FRP data corresponding to different fire clusters (2010) is

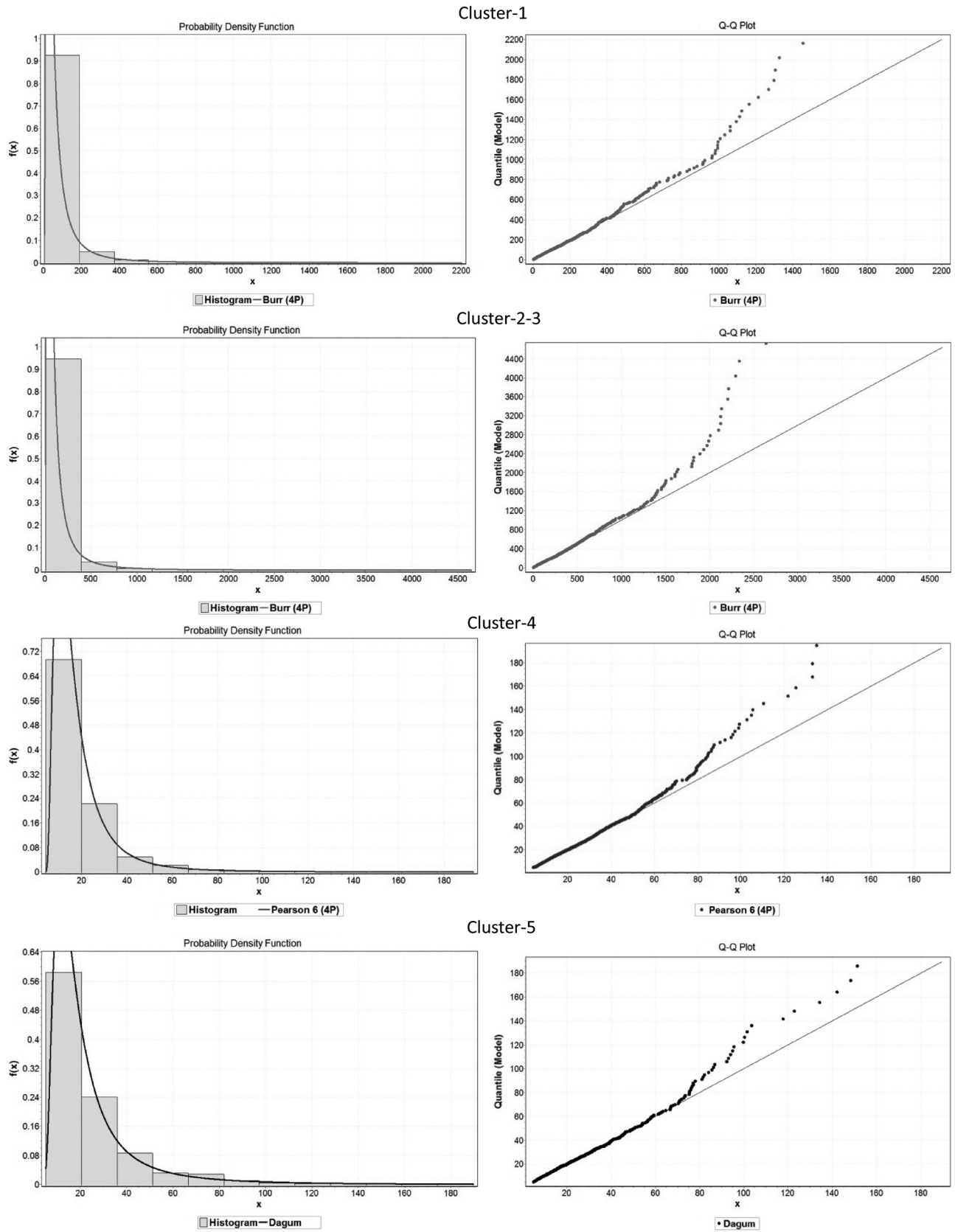


Fig. 6. (a)–(g) Probability density distributions fitted for the FRP data(x) in different clusters along with the Q-Q plots.

shown in Fig. 7. These plots were used to assess the relative strength of FRP values based on percentile data falling below or above the median. For example, the median FRP value for fire cluster 1 is 30.9 MW. The 90th percentile shows that 90% of the

FRP values in this cluster are smaller than 153.5 MW (Fig. 5(a)). Similarly, for cluster 4 dominated by agricultural fires, the median FRP was 15.3 MW and the 90th percentile values fell below 35.7 MW (Fig. 7). Thus, comparison of the above two clusters

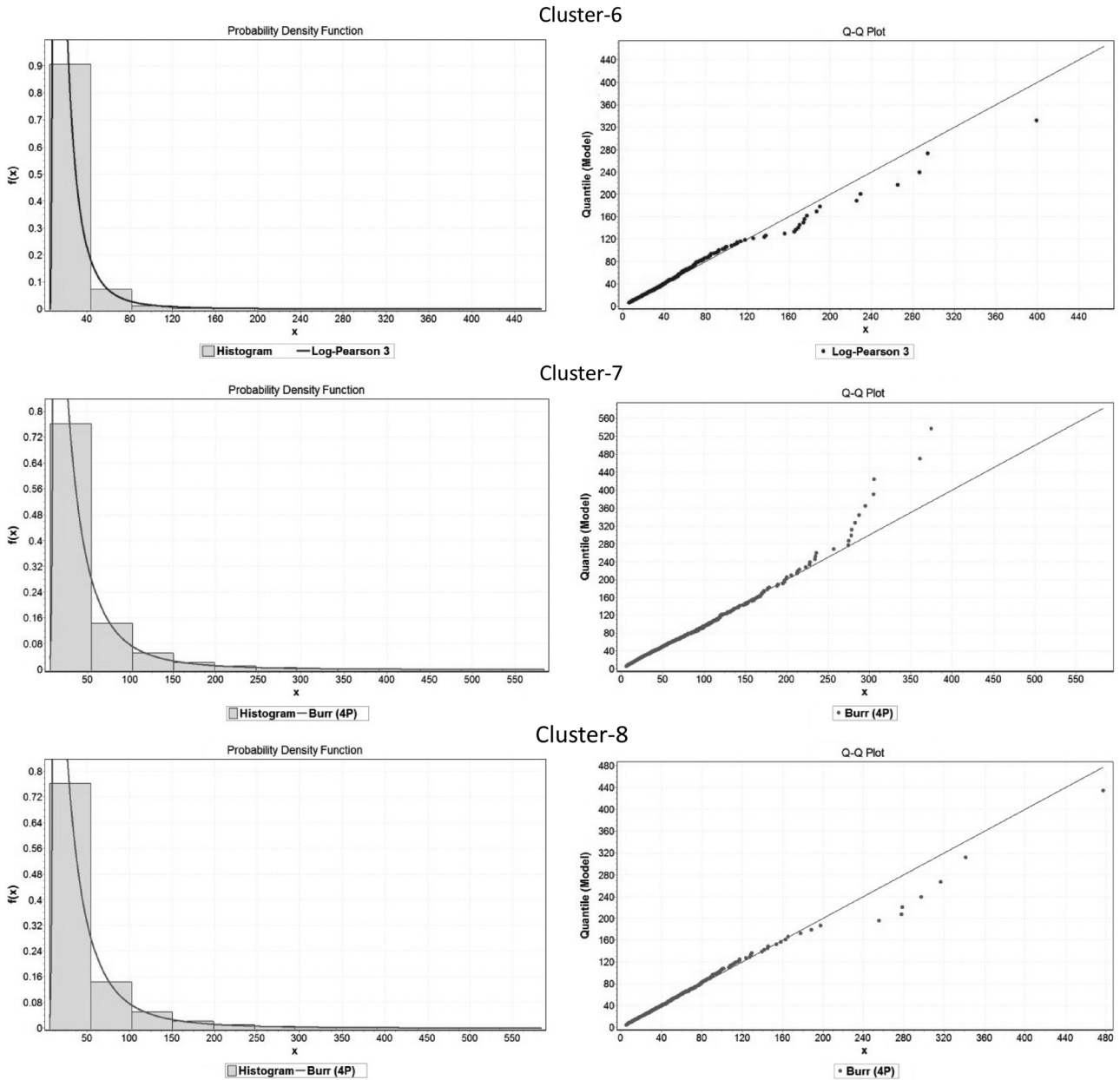


Fig. 6. (Continued).

(1 versus 4) clearly suggests cluster 1 had higher FRP values compared to cluster 6. In all, comparison of median FRP values across the plots suggests that FRP was considerably high for 1 and 2–3 clusters corresponding to northeast India compared to the others. In general for all the data, the mean FRP is greater than the median, thus the FRP data mostly showed positive skew towards the right side, however, the difference between the mean and median is considerably smaller for cluster 4 corresponding to agricultural fires than the other clusters. Cluster 6 dominated by the broadleaved deciduous forests had higher median FRP than the agricultural fires (cluster 4); however, the values were less than closed to open broadleaved evergreen or semi-deciduous forests of northeastern India.

FRP data in fire cluster 7 which is dominated by irrigated croplands and mosaic cropland category showed median and 90th percentile FRP values higher than the other agricultural fires (cluster four) and closed broadleaved deciduous forests

(cluster six). It is interesting to note that median FRP values in cluster 8 with the mosaic cropland/vegetation category (30.5%), rainfed croplands (19.1%) and closed broadleaved deciduous forests (18.1%) had a relatively higher median FRP than the cluster 6 dominated by broadleaved deciduous forests category. Further, the 90th percentile values in this cluster (eight) are also higher (145.8 MW) than the cluster six. In summary, results from cdf plots suggest the median FRP values in the following relative order a) high values for a closed to open broadleaved evergreen or semi-deciduous forests pertaining to northeast India; b) medium FRP in mosaic vegetation types (clusters seven and eight); c) low FRP in closed broadleaved deciduous forest category (cluster six); d) very low FRP values in the irrigated cropland category (cluster four).

In addition to the cdf plots, we also used annual sum of FRP (A-FRP) estimates over different fire clusters to assess which fires burn more intensively over a period of time (Fig. 4(i)).

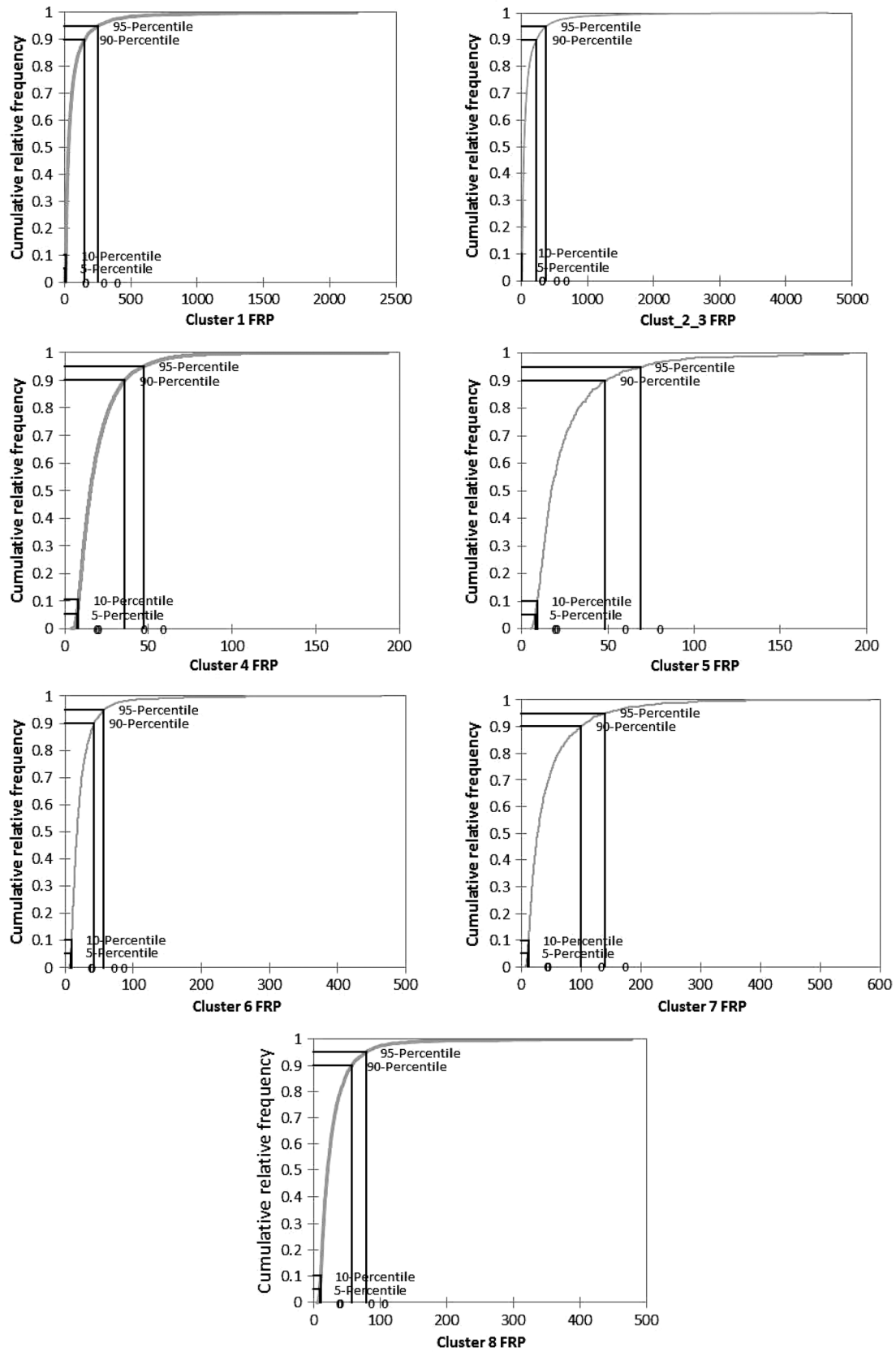


Fig. 7. (a)–(g) Empirical cumulative distribution function plots of FRP data in different clusters.

Fire intensities are governed by a variety of factors, the most important factor being vegetation type. Results clearly suggest fires in the cluster 2–3 and one dominated by closed broadleaved evergreen or semi-deciduous forest burn more intensively than

the other vegetation types (Fig. 4(i)). These results were contrary to our initial hypothesis that A-FRP released from the broadleaved deciduous forests will be much higher than the evergreen forests. Our hypothesis that A-FRP release in trop-

ical dry deciduous forests will be higher than the evergreen forests was primarily based on the meteorological factors, i.e., the drier the vegetation, the higher the fire proneness and possibly larger fire counts resulting in higher A-FRP release. However, the causative factors of fires seem mostly anthropogenic rather than meteorological factors in India. For example, the fires in the northeast India (cluster 1, 2–3) mostly pertain to slash and burn agriculture [43], [44]. Thus cluster 1, and 2–3 had the highest number of fire counts after agricultural fires (Cluster 4). These regions are also characterized by the high fuel loads compared to deciduous forests (cluster six) [45], [46]. Thus, higher fire counts together with higher fuel loads in these clusters contributed to higher A-FRP.

Relating to the second hypothesis that A-FRP released from agricultural residue burning will be much less than the forest fires, the results varied based on the forest type. For example, as hypothesized, the A-FRP for the agricultural residue fires (cluster 4) was considerably less than the closed broadleaved evergreen forests (clusters 1, 2–3). However, A-FRP was considerably higher for agricultural residue fires (cluster 4), compared to the mosaic vegetation category clusters (7 and 8), and cluster 6 dominated by the broadleaved deciduous forest category (Fig. 4(i)). Further, monthly variations in FRP revealed quite different patterns based on the type of vegetation burnt and geographical regions. Peak FRP is found to be high during March for clusters 1, 2–3, 8, 6 (Fig. 4(d), (f), (h), (g)), whereas cluster 5 and 7 had the peak during April (Fig. 4(c), (e)). In contrast to all the other fire clusters, cluster 4 dominated by agricultural fires had A-FRP peak during November (Fig. 4(b)). Our earlier study on agricultural residue fires in the cluster four region clearly suggest that fires during winter (October–November) correspond to rice residue burning events and fires during summer (March–May) to wheat residue burning in that region [42]. These results on FRP over different geographical regions can be useful to retrieve biomass combustion rates in different ecosystems [47], [48], quantifying trace gases, smoke and aerosol emissions [29], [50], [51] and consequently for understanding the impact of vegetation fires on air pollution and climate. In addition, information on the FRP can also be used to infer biomass and bioenergy relationships for addressing renewable energy questions.

IV. CONCLUSIONS

Spatial patterns in fire occurrences and intensity in India has been analyzed using MODIS fire datasets. MODIS data was quite useful in characterizing spatial patterns in fire occurrences as well as some fire regime attributes. K-means clustering technique was useful in identifying hotspot regions of fire clusters. Using the fire radiative power (FRP) data, we analyzed the fire intensity in hotspot clusters using distribution fitting and cumulative distribution function plots. We also tested two different hypotheses, first, amongst different forest types, annual sum of FRP (A-FRP) released from the closed broadleaved deciduous forests will be much higher compared to the closed to open broadleaved evergreen forests; second, due to the lower fuel loads in agricultural systems compared to forests, the agricultural residue fires will have lower A-FRP values than the forest fires. Results suggested a variety of statistical distribution types

for the FRP data based on the type of vegetation burnt, the most common being Burr distribution. Analysis from empirical cumulative distribution plots suggested relatively high fire intensity for closed broadleaved evergreen/semi-deciduous forests than the other vegetation types. Contrary to our first hypothesis, results suggested that A-FRP released from broadleaved evergreen forests is much higher than the other vegetation types. This is mainly attributed to anthropogenic nature of fires in the region compared to meteorological factors. Relating to the second hypothesis, A-FRP of the agricultural fires compared to forests varied based on the vegetation type burnt and the total number of fire counts. Agricultural fires were found to have significantly higher A-FRP due to higher fire counts (large number of fires) than the mosaic vegetation category and broadleaved deciduous forests. In summary, results from this study highlight spatial variations in fire intensities and geographical regions of fire hotspots useful for addressing fire management issues and pollution aspects in India.

ACKNOWLEDGMENT

The authors thank the editors and anonymous reviewers for providing useful comments and suggestions.

REFERENCES

- [1] M. A. Fosberg, L. O. Mearns, and C. Price, "Climate change—Fire interactions at the global scale: Predictions and limitations of methods," in *Fire in the Environment: The Ecological, Atmospheric and Climatic Importance of Vegetation Fires*, P. Crutzen and J. G. Goldammer, Eds. New York: Wiley, 1993, pp. 125–137.
- [2] M. G. Schultz, "On the use of ATSR fire count data to estimate the seasonal and interannual variability of vegetation fire emissions," *Atmos. Chem. Phys.*, vol. 2, pp. 387–395, 2002.
- [3] E. Chuvieco, J. Wagtenok, D. Riano, M. Yebra, and S. L. Ustin, "Estimation of fuel conditions for fire danger assessment," in *Earth Observation of Wildland Fires in Mediterranean Ecosystems*. Springer, 2009, p. 14.
- [4] P. R. Dansereau and Y. Bergeron, "Fire history in the southern boreal forest of Quebec," *Canadian J. Forest Research*, vol. 23, pp. 25–32, 1993.
- [5] K. Paliwal and V. M. Sundaravalli, "Effect of fire on nutrient dynamics in a semiarid grazing land ecosystem of Madurai," *Current Science*, vol. 83, pp. 316–318, 2002.
- [6] M. G. Turner and W. H. Romme, "Landscape dynamics in crown fire ecosystems," *Landscape Ecol.*, vol. 9, pp. 59–77, 1994.
- [7] S. Roberts, "Tropical fire ecology," *Progress in Physical Geography*, vol. 24, pp. 281–288, 2000.
- [8] S. J. Pyne, "How Plants Use Fire (And Are Used By It)," PBS NOVA Online, Jan. 1, 2006 [Online]. Available: <http://www.pbs.org/wgbh/nova/fire/plants.html>, 2002
- [9] R. J. Vogl, "Effects of fire on grasslands," in *Fire in Ecosystems*, T. T. Kozlowski and C. E. Ahlgren, Eds. New York: Academic Press, 1974, pp. 139–194.
- [10] F. Guerra, H. Puig, and R. Chaume, "The forest-savanna dynamics from multi-date Landsat(TM) data in Sierra Parima, Venezuela," *Int. J. Remote Sens.*, vol. 11, pp. 2061–2075, 1998.
- [11] H. Eva and E. Lambin, "Fires and land-cover change in the tropics: A remote sensing analysis at the landscape scale," *J. Biogeography*, vol. 27, pp. 765–776, 2000.
- [12] P. J. Crutzen and M. O. Andreae, "Biomass burning in the tropics—Impact on atmospheric chemistry and biogeochemical cycles," *Science*, vol. 250, no. 4988, pp. 1669–1678, 1990.
- [13] G. R. van der Werf, J. T. Randerson, L. Giglio, G. J. Collatz, M. Mu, P. S. Kasibhatla, D. C. Morton, R. S. DeFries, Y. Jin, and T. T. van Leeuwen, "Global fire emissions and the contribution of deforestation, savanna, forest, agricultural, and peat fires (1997–2009)," *Atmos. Chem. Phys.*, vol. 10, pp. 11707–11735, 2010.
- [14] W. K. M. Lau, M. K. Kim, and W. S. Lee, "Enhanced surface warming and accelerated snow melt in the Himalayas and Tibetan Plateau induced by absorbing aerosols," *Environ. Res. Lett.*, vol. 5, pp. 1–10.

- [15] M. A. Gill and G. Allan, "Large fires, fire effects and the fire-regime concept," *Int. J. Wildland Fire*, vol. 17, pp. 688–695, 2008.
- [16] T. L. Swetnam and P. M. Brown, "Comparing selected fire regime condition class (FRCC) and LANDFIRE vegetation model results with tree-ring data," *Int. J. Wildland Fire*, vol. 19, no. 1, pp. 1–13, 2010, 10.1071/WF08001.
- [17] R. J. Barney and B. J. Stocks, "Fire frequencies during the suppression period," in *The Role of Fire in Northern Circumpolar Ecosystems*, R. W. Wein and D. A. MacLean, Eds. New York: Wiley, 1983, pp. 45–62.
- [18] E. S. Kasischke, J. H. Hewson, B. Stocks, and G. van der Werf, "The use of ATSR active fire counts for estimating relative patterns of biomass burning—A study from the boreal forest region," *Geophys. Res. Lett.*, vol. 30, no. 18,969, pp. 1–4, 2003, 10.1029/2003GL017859.
- [19] L. F. DeBano, D. G. Neary, and P. F. Ffolliot, *Fire's Effects on Ecosystems*. New York: Wiley, 1998.
- [20] B. W. Duncan and P. A. Schmalze, "Anthropogenic influences on potential fire spread in a pyrogenic ecosystem of Florida, USA," *Landscape Ecology*, vol. 19, pp. 153–165, 2004.
- [21] A. Leone, C. Perrotta, and B. Maresca, "Plant tolerance to heat stress: Current strategies and new emergent insight," in *Abiotic Stresses in Plants*, L. Sanita di Toppi and B. Pawlik-Skowronska, Eds. Dordrecht, The Netherlands: Kluwer Academic, 2003, pp. 1–22.
- [22] B. W. Duncan, G. Shao, and F. W. Adrian, "Delineating a managed fire regime and exploring its relationship to the natural fire regime in East Central Florida, USA: A remote sensing and GIS approach," *Forest Ecology and Management*, vol. 258, no. 2, pp. 132–145, 2009.
- [23] V. K. Bahuguna and A. Upadhyay, "Forest fires in India: Policy initiatives for community participation," *Int. Forestry Review*, vol. 4, no. 2, pp. 122–127, 2002.
- [24] State of the Forest Report. India-State of the Forest Report. Forest Survey of India, Ministry of Environment and Forests, Government of India, Dehradun, India, 2001.
- [25] D. K. Davies, S. Illavajhala, M. M. Wong, and C. O. Justice, "Fire information for resource management system: Archiving and distributing MODIS active fire data," *IEEE Trans. Geosci. Remote Sens.*, vol. 47, no. 1, pp. 72–79, 2009.
- [26] L. Giglio, J. Desloitures, C. O. Justice, and Y. Kaufman, "An enhanced contextual fire detection algorithm for MODIS," *Remote Sens. Environ.*, vol. 87, pp. 273–282, 2003.
- [27] Y. J. Kaufman, C. O. Justice, L. Flynn, J. D. Kendall, E. M. Prins, L. Giglio, D. Ward, W. Menzel, and A. Setzer, "Potential global fire monitoring from EOS-MODIS," *J. Geophys. Res.*, vol. 103, pp. 32215–32238, 1998.
- [28] M. J. Wooster and Y. H. Zhang, "Boreal forest fires burn less intensely in Russia than in North America," *Geophys. Res. Lett.*, vol. 31, no. L20505, 2004, 10.1029/2004GL020805.
- [29] E. Vermote, E. Ellicott, O. Dubovik, T. Lapyonok, M. Chin, L. Giglio, and G. J. Roberts, "An approach to estimate global biomass burning emissions of organic and black carbon from MODIS fire radiative power," *J. Geophys. Res.*, vol. 114, 2009, 10.1029/2008jd011188.
- [30] L. Giglio, MODIS Collection 5 Active Fire Product User's Guide: Version 2.4. [Online]. Available: http://modis-fire.umd.edu/documents/MODIS_Fire_Users_Guide_2.4.pdf (last accessed 12th June, 2011), 2010
- [31] P. Bicheron, V. Amberg, L. Bourg, D. Petit, M. Huc, B. Miras, C. Brockmann, S. Delwart, F. Ranéra, O. Hagolle, M. Leroy, and O. Arino, 2008, Geolocation Assessment of 300 m Resolution MERIS Globcover Ortho-Rectified Products. [Online]. Available: http://postel.mediasfrance.org/IMG/pdf/Bicheron_etal_MERISColloque_sept2008.pdf
- [32] L. Kaufman and P. J. Rousseeuw, *Finding Groups in Data: An Introduction to Cluster Analysis*. New York: Wiley, 1990, 342p.
- [33] W. D. Fisher, "On grouping for maximum homogeneity," *J. Amer. Statist. Assoc.*, vol. 53, no. 789–98, 1958.
- [34] J. MacQueen, "Some methods for classification and analysis of multivariate observations," in *Proc. 5th Berkeley Symp. Math and Statistics Problems*, 1967, vol. 1, pp. 281–297.
- [35] J. A. Hartigan and M. A. Wong, "A K-means clustering algorithm," *Applied Statistics*, vol. 28, pp. 100–108, 1978.
- [36] V. Estivill-Castro and A. T. Murray, "Hybrid optimization for clustering in data mining," in *Proc. X CLAI/O, X Latin-Ibero-American Conf. Operations Research and Systems*, Mexico City, Mexico, Sep. 2000, Paper A168, CD-ROM.
- [37] A. J. Brimicombe, *GIS, Environmental Modelling and Engineering*. London, U.K.: Taylor & Francis, 2003.
- [38] H. J. Miller and J. Han, *Geographic Data Mining and Knowledge Discovery*. London, U.K.: Taylor and Francis, 2001, pp. 337–361.
- [39] N. Levine, CrimeStat: A Spatial Statistics Program for the Analysis of Crime Incident Locations (v. 3.3), Ned Levine & Associates, Houston, TX, and the National Institute of Justice, Washington, DC., Jul. 2010.
- [40] Mathwave, 2011 [Online]. Available: <http://www.mathwave.com/en/home.html>
- [41] P. K. Gupta, S. Sahai, N. Singh, C. K. Dixit, D. P. Singh, C. Sharma, M. K. Tiwari, R. K. Gupta, and S. C. Garg, "Residue burning in rice-wheat cropping system: Causes and implications," *Current Science*, vol. 87, no. 12, pp. 1713–1717, 2004.
- [42] K. P. Vadrevu, E. Ellicott, K. V. S. Badarinath, and E. Vermote, "MODIS derived fire characteristics and aerosol optical depth variations during the agricultural residue burning season, North India," *Environmental Pollution*, vol. 159, pp. 1560–1569, 2011.
- [43] P. S. Ramakrishnan, "Sustainable development, climate change and tropical rain forest landscape," *Climatic Change*, vol. 39, pp. 583–600, 1988.
- [44] M. Majumder, A. K. Shukla, and A. Arunachalam, "Agricultural practices in Northeast India and options for sustainable management. Biodiversity, biofuels, agroforestry and conservation agriculture," *Sustainable Agriculture Reviews*, vol. 5, pp. 287–315, 2011, 10.1007/978-90-481-9513-8-10.
- [45] S. C. Garkoti and S. P. Singh, "Variation in net primary productivity and biomass of forests in the high mountains of Central Himalaya," *J. Vegetation Science*, vol. 6, no. 1, pp. 23–28, 2009.
- [46] R. Baishya, S. K. Bari, and K. Upadhaya, "Distribution pattern of aboveground biomass in natural and plantation forests of humid tropics in Northeast India," *Tropical Ecology*, vol. 50, no. 2, pp. 295–304, 2009.
- [47] M. J. Wooster, G. Roberts, G. L. W. Perry, and Y. J. Kaufman, "Retrieval of biomass combustion rates and totals from fire radiative power observations: FRP derivation and calibration relationships between biomass consumption and fire radiative energy release," *J. Geophys. Res.*, vol. 110, no. D24311, 2005, 10.1029/2005JD006318.
- [48] G. Roberts, M. J. Wooster, G. L. Perry, N. Drake, L. M. Rebelo, and F. Dipotso, "Retrieval of biomass combustion rates and totals from fire radiative power observations: Application to southern Africa using geostationary SEVIRI imagery," *J. Geophys. Res.*, vol. 110, no. D21111, 2005.
- [49] R. E. Burgan, R. W. Klaver, and J. M. Klaver, "Fuel models and fire potential from satellite and surface observations," *Int. J. Wildland Fire*, vol. 8, pp. 159–170, 1998.
- [50] C. Ichoku and Y. J. Kaufman, "A method to derive smoke emission rates from MODIS fire radiative energy measurements," *IEEE Trans. Geosci. Remote Sens.*, vol. 11, no. 43, pp. 2636–2649, 2005.
- [51] G. Pereira, S. R. Freitas, E. C. Moraes, J. E. Ferreira, Y. E. Shimabukuro, V. B. Rao, and K. M. Longo, "Estimating trace gas and aerosol emissions over South America: Relationship between fire radiative energy released and aerosol optical depth observations," *Atmospheric Environment*, vol. 43, pp. 6388–6397, 2009.
- [52] A. Sarkargar, V. Zoj, A. Mohammadzadeh, M. J. Mansourian, and A. , "Spatial and temporal analysis of fires detected by MODIS data in Northern Iran from 2001 to 2008," *IEEE J. Sel. Topics Appl. Earth Observ. Remote Sens. (JSTARS)*, 2010, 10.1109/JSTARS.2010.2088111.
- [53] M. S. Akther and Q. K. Hassan, "Remote sensing-based assessment of fire danger conditions over boreal forest," *IEEE J. Sel. Topics Appl. Earth Observ. Remote Sens. (JSTARS)*, vol. 4, pp. 992–999, 2011.
- [54] U. M. Fayyad, G. Piatetsky-Shapiro, P. Smyth, and R. Uthurusamy, *Advances in Knowledge Discovery and Data Mining*. Cambridge, MA: AAAI/MIT Press, 1996.
- [55] A. Gersho and R. M. Gray, *Vector Quantization and Signal Compression*. Boston, MA: Kluwer Academic, 1992.
- [56] R. O. Duda and P. E. Hart, *Pattern Classification and Scene Analysis*. New York: Wiley, 1973.
- [57] G. Punj and D. W. Stewart, "Cluster analysis in marketing research: Review and suggestions for application," *J. Marketing Research*, vol. XX, pp. 134–48, May 1983.
- [58] A. T. Murray, I. McGuffoc, J. S. Western, and P. Mullins, "Exploratory spatial data analysis techniques for examining urban crime. 2001," *Brit. J. Criminology*, vol. 41, pp. 309–329, 2001.
- [59] Z. Munch, S. W. P. Van Lill, C. N. Booyesen, H. L. Zietsman, D. A. Enarson, and N. Beyers, "Tuberculosis transmission patterns in a high-incidence area: A spatial analysis," *Int. J. Tuberculosis and Lung Disease*, vol. 7, no. 3, pp. 271–277(7), 2003.
- [60] Y. Xu, V. Olman, and D. Xu, "Clustering gene expression data using a graph-theoretic approach: An application of minimum spanning trees," *Bioinformatics*, vol. 18, no. 4, pp. 536–545, 2002.
- [61] T. K. Anderson, "Kernel density estimation and K-means clustering to profile road accident hotspots," *Accident Analysis and Prevention*, vol. 41, no. 3, pp. 359–364, 2009.

- [62] U. N. Kanjilal, P. C. Kanjilal, and A. Das, *Flora of Assam Series*. Dehradun, India: Allied Book Centre, 1991.
- [63] K. P. Vadrevu, E. Ellicott, L. Giglio, K. V. S. Badarinath, E. Vermote, C. Justice, and B. Lau, "Vegetation fires in the Himalayan Region—Aerosol load, black carbon emissions and smoke plume heights," *Atmospheric Environment*, vol. 47, pp. 241–251, 2012.
- [64] V. K. Prasad, Y. Kant, P. K. Gupta, C. Sharma, A. P. Mitra, and K. V. S. Badarinath, "Biomass and combustion characteristics of secondary mixed deciduous forests in Eastern Ghats of India," *Atmospheric Environment*, vol. 35, pp. 3085–3095, 2001.



Krishna Prasad Vadrevu received the Ph.D. degree in ecology and remote sensing in 2000 while working at the Indian Space Research Organization (ISRO), National Remote Sensing Center, Hyderabad, India. His thesis focused on biodiversity and forest characterization using remote sensing techniques.

From 2001–2003, he worked as a postdoctoral researcher and 2004–2009 as a research scientist at the Ohio State University, USA. Since 2010, he is working as an Associate Research Professor at the department of Geographical Sciences, University of

Maryland, College Park. His research has been highly interdisciplinary. His publications are in biomass burning, greenhouse gas emission inventories, carbon cycling, land use/cover change studies, agroecosystems, spatial statistics, etc. At the University of Maryland, he is focusing on the fire research. He is also the Fire Implementation Team Executive officer for the Global Observation of Forest and Land Cover Dynamics (GOF-C-GOLD), Fire Mapping and Monitoring Program.



Ivan Csizsar received the Ph.D. in 1996 in earth sciences from the Eötvös Loránd University in Budapest, Hungary. His early research focused on atmospheric sounding and on the retrieval of cloud optical and microphysical properties. He has also worked on the retrieval of land surface properties.

His current research focuses on satellite-based fire detection and monitoring. He has led several NASA-funded research projects aimed at fire mapping and evaluating fire products and impacts, including products from the Advanced Very High

Resolution Radiometer (AVHRR), the Moderate Resolution Imaging Spectroradiometer (MODIS) and the Visible Infrared Imager Radiometer Suite (VIIRS). He has been an active contributor to the Fire component of the GOF-C-GOLD program and Group on Earth Observations (GEO). Currently, he is the chief of the Environmental Monitoring Branch, Satellite meteorology and climatology division, NOAA/NESDIS Center for Satellite Applications and Research, Camp Springs, Maryland, USA.



Evan Ellicott received the Ph.D. in geography from the University of Maryland, College Park, in 2009.

His research interests include satellite based estimates of fire radiative energy and associated biomass burning emissions; Fire ecology and consequences of a changing climate and land cover and land use change, in particular the interrelationships with climate and sustainability. Currently, he is working as an Assistant Research Professor at the department of Geographical Sciences, University of Maryland College Park, USA.



Louis Giglio received the B.S. degree in physics from the University of Maryland at College Park (USA), the M.S. degree in applied physics from The Johns Hopkins University, Baltimore, Maryland, and the Ph.D. in geography, again from the University of Maryland at College Park, where he is currently a Research Associate Professor in the Department of Geographical Sciences.

His research interests include remote sensing of active fires and burned area on a global scale, global fire emissions, and satellite direct broadcast applications.



K. V. S. Badarinath received the Ph.D. in physics from the Indian Institute of Technology, India, in 1984. He worked as the head, atmospheric science section, National Remote Sensing Agency, Hyderabad, India, until recently (2011). For over three decades, he focused on remote sensing applications, atmospheric aerosols, and vegetation fires. He brought the fire and aerosol instrumentation research in India to new heights. He was a Fellow of Indian Geophysical Union and Andhra Pradesh Academy of Sciences, India. He was also GOF-C-GOLD

Fire-Implementation team member. He published several research papers in national and international journals and supervised nine Ph.D. students. We are saddened by his sudden demise (January, 2012).



Eric Vermote received the Ph.D. in 1990 in atmospheric optics from the University of Lille, France.

He is currently a Research Professor in the Department of Geographical sciences, University of Maryland, College Park. His research interests are in radiative transfer modeling, vicarious calibration, atmospheric correction, aerosol retrieval, and the generation of climate data record for terrestrial studies.

Dr. Vermote is a member of the Moderate Resolution Imaging Spectroradiometer Science Team, the NASA National Polar-orbiting Operational Environmental Satellite System Preparatory Project Science Team for the VIIRS sensor, the Landsat Data Continuity Mission Science Team, and is responsible for the atmospheric correction over land surfaces in the visible-to-middle infrared.



Chris Justice received the Ph.D. in geography from the University of Reading, Reading, U.K., in 1977.

In 2001, he became Professor and Research Director in the Department of Geographical Sciences, University of Maryland College Park and since 2010, he has been serving as the Department Chair. He is a member of the NASA Moderate Imaging Spectroradiometer (MODIS) Science Team and is responsible for the MODIS Fire Product. He is the Co-Chair for the NASA LANCE User Working Group, the GOF-C-GOLD-Fire Implementation

Team as well as the GEO Global Agricultural Monitoring Task. He is a member of the NASA JPSS/NPOESS Preparatory Project (NPP) Science Team. He is also a P.I. for USAID's Central Africa Regional Project for the Environment. He is the NASA Land Cover Land Use Change Program Scientist. His current research is on land cover and land use change, the extent and impacts of global fire, global agricultural monitoring, and their associated information technology and decision support systems.